Photoelectrodes

DOI: 10.1002/ange.201406044

Switchable Charge-Transfer in the Photoelectrochemical Energy-Conversion Process of Ferroelectric $BiFeO_3$ Photoelectrodes**

*Dawei Cao, Zhijie Wang, Nasori, Liaoyong Wen, Yan Mi, and Yong Lei**

Abstract: *Instead of conventional semiconductor photoelectrodes, herein, we focus on $BiFeO_3$ ferroelectric photoelectrodes to break the limits imposed by common semiconductors. As a result of their prominent ferroelectric properties, the photoelectrodes are able to tune the transfer of photo-excited charges generated either in $BiFeO_3$ or the surface modifiers by manipulating the poling conditions of the ferroelectric domains. At 0 V vs Ag/AgCl, the photocurrent could be switched from 0 $\mu A\,cm^{-2}$ to 10 $\mu A\,cm^{-2}$ and the open-circuit potential changes from 33 mV to 440 mV, when the poling bias of pretreatment is manipulated from −8 V to +8 V. Additionally, the pronounced photocurrent from charge injection of the excited surface modifiers could be quenched by switching the poling bias from +8 V to −8 V.*

As the only active materials in the photovoltaic and photoelectrochemical cells for solar-energy conversion, conventional semiconductors have been studied thoroughly for the past several decades.[1–4] The aim of technologies in semiconductor device fabrication is to attain energy-conversion efficiency close to the theoretical values based on the band gap analysis of the semiconductors.[5,6] The current approach for energy-conversion devices with traditional semiconductors, however, has two limits: 1) the photovoltage of the devices is limited by the band gap of the semiconductors employed ; 2) the charge-transfer direction is confined and fixed by the junctions of the semiconductor/semiconductor, semiconductor/metal or semiconductor/electrolyte.

An alternative approach to overcome the limits of the common semiconductors is to fabricate solar-energy conversion devices with ferroelectric materials. Ferroelectric materials, typically $BiFeO_3$ (BFO)[7–11] and $Pb(Zr,Ti)O_3$ (PZT),[12–14] have a large, stable and tunable remnant ferroelectric polarization which produces a depolarization (internal) electric field extending over the whole film volume, giving the resulting devices high efficiency in separating photo-generated charges and switching charge-transfer directions. Therefore, Walsh et al.[15] claimed that the excellent performance of Perovskite solar cells based on $CH_3NH_3PbI_3$ originated from the presence of ferroelectric domains in the Perovskite structure. Ferroelectric materials also exhibit unique abnormal photovoltaic effects. By controlling the conductivity of the ferroelectric domain walls, the detected open-circuit potential (V_{oc}) for a standard ferroelectric material, BFO, has been as high as 50 V,[10] more than 50-fold larger than that from regular Si solar cells, indicative of that a huge V_{oc} from ferroelectric materials is achievable even without considering the band-gap limit. In addition, the orientation and intensities of the internal field could be manipulated by external applied voltages and the ferroelectric materials can theoretically maintain the remnant polarization permanently in an inert condition,[16–19] implying that a single ferroelectric photoelectrode could be treated as both a photocathode and a photoanode depending on the orientations of the internal field. Consequently, it is highly realizable that a ferroelectric photoelectrode with an appropriate band gap can serve to drive both water reduction and oxidation reactions just by tuning the remnant polarization directions, which is extremely important in photoelectrochemistry. Moreover, by getting rid of the top Schottky barrier at the contact between the ferroelectric material and metal that generally exists in the ferroelectric photovoltaic devices,[8,12] the ferroelectric photoelectrochemical electrodes have a better capability in extracting the photo-excited charges and are compatible with with other promising photo-active materials, unlike the solid-state counterpart.

To date most of the efforts on the application of ferroelectric materials to solar-energy conversion are confined to solid-state solar cells and few reports concern the photoelectrochemical performance of the ferroelectric materials.[14,20,21] A systematic study of this area is thus indispensable to promote the evolution of photoelectrochemical energy conversion/storage. Instead of using PZT (band gap: 3.5 eV[12,13]) as the photoelectrode, herein, we choose another typical ferroelectric material, BFO (band gap: 2.2 eV[11,22]). The lower band gap of BFO makes it possible to form a good band-gap alignment with surface modifiers that could inject excited charges to the BFO photoelectrodes. Surprisingly, we found that the charge transfer from the bare BFO to the electrolyte and from the surface modifiers to BFO could be manipulated by the poling pretreatment. A series of surface modifiers, such as molecular dyes and CdSe quantum dots, was investigated and provides strong support that ferro-

[*] Dr. D. Cao,[+] Dr. Z. Wang,[+] Nasori, L. Wen, Y. Mi, Prof. Y. Lei
Institut für Physik & IMN MacroNano®(ZIK)
Technische Universität Ilmenau
98693 Ilmenau (Germany)
E-mail: yong.lei@tu-ilmenau.de
Prof. Y. Lei
Institute of Nanochemistry and Nanobiology, Shanghai University
200444 Shanghai (P. R. China)

[+] These authors contributed equally to this work.

[**] This work was financially supported by European Research Council (ThreeDsurface: 240144), BMBF (ZIK-3DNanoDevice: 03Z1MN11), Volkswagen-Stiftung (Herstellung funktionaler Oberflächen: I/83 984), Shanghai Thousand Talent Plan and Innovative Research Team (No. IRT13078).

Supporting information for this article is available on the WWW under http://dx.doi.org/10.1002/anie.201406044.

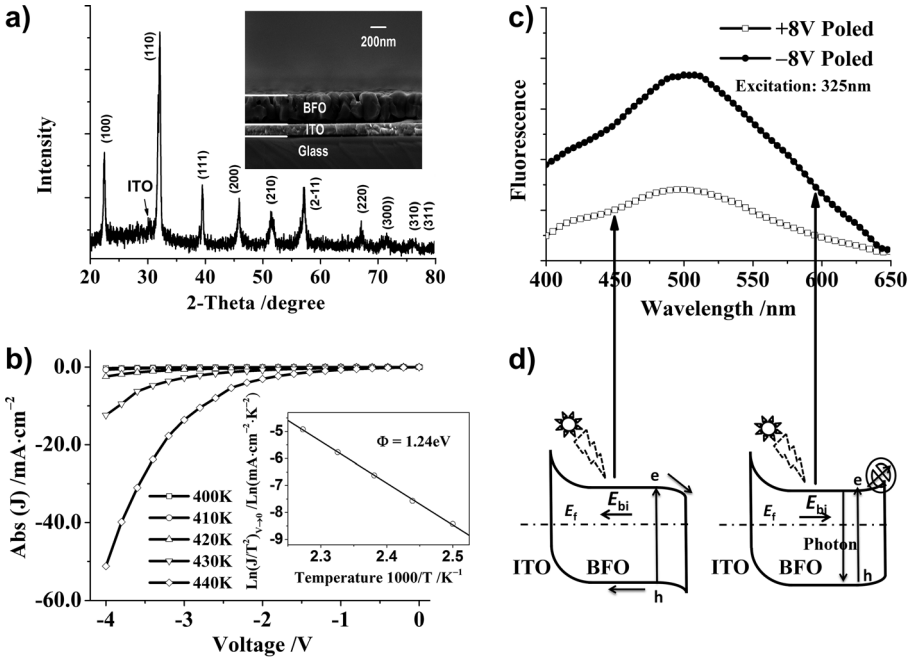

Figure 1. a) XRD pattern of the BFO films (Inset: cross-sectional SEM). b) Dark *J–V* plots of the structure: Au/BFO/ITO (Inset: fitting to Schottky–Simmons equation). c) The fluorescence spectra and d) schematic representation of energy band-gap alignment of the BFO/ITO after poling of +8 V and −8 V, respectively.

electric photoelectrodes are the right candidates for the next generation photoelectrochemical electrodes.

Rather than growing BFO films epitaxially by radio-frequency (RF) magnetron sputtering or pulsed-laser deposition (PLD),[8,10] we adopted a cost-advantageous technology, spin-coating, to obtain high-quality BFO films on ITO/glass.[23] Preparation details and a description of the methods employed for data collection are provided in the Supporting Information. Figure 1 a presents the X-ray diffraction (XRD) pattern of the polycrystalline BFO films on ITO-coated glass substrate, where the diffraction peaks at 2θ values of 22.48, 31.89, and 39.18 could be indisputably ascribed to the reflection of (100), (110), and (111) planes of BFO (JCPDS card No.72-2112), respectively. No diffraction signatures of $Bi_2Fe_4O_9$ and Bi_2O_3/Fe_2O_3 are observed, suggesting that the as-prepared BFO films possess a pure Perovskite structure. Additionally, consistent with other reports,[11,22] the energy band gap of the BFO film was characterized as 2.14 eV by the absorption spectroscopy shown in Figure S1, indicating that it is a superior material for photoelectrochemistry than its counterparts, such as PZT and $BaTiO_3$.[24,25]

The cross-sectional scanning electron micrograph (SEM) of the spin-coated BFO thin film on ITO/glass, allows the thicknesses of BFO and ITO to be gauged as about 300 nm and 100 nm, respectively (Figure 1 a). The BFO/ITO interface is of high prominence visually, suggesting that this electronic junction should probably play a significant role in the photoelectrochemical performance. Thus, the BFO/ITO junction was investigated and the relevant data are illustrated in Figure 1 b. On the basis of the dark *J–V* analyses of the Au/BFO/ITO devices under various temperatures and the fitting of Schottky–Simmons equation (Figure 1 b), it is demonstrated that the BFO/ITO contact is a typical Schottky junction and the electronic barrier height for BFO/ITO is estimated to be around 1.24 eV, in agreement with reported values.[26] The measurement and analytical details can be found in the Supporting Information. Yang et al. and Schafranek et al.[26,27] reported that the Schottky height in the metal/ferroelectric film was mainly determined by the interfacial charge percentage, which is related to interfacial defects such as oxygen vacancies generated in the annealing procedures. Accordingly, such a Schottky barrier could not be changed reversely by poling treatments, thus we can focus on the contact between the BFO and the electrolyte.

Though the ferroelectric properties of the spin-coated BFO thin films are not comparable with the films prepared by high-vacuum techniques, a set of *P–E* hysteresis loops as a function of test voltages in Figure S2 still clearly indicates the existence of the ferroelectric hysteresis in the samples, providing us with a cost-efficient platform to tune the internal electric field induced by the remnant polarization and thus to manipulate the charge transfers of the photoelectrochemistry. Steady-state fluorescence spectroscopy is a convenient methodology to analyze photo-generated charge-transfer dynamics. Before fluorescent measurements, the BFO electrodes were pretreated electrochemically in a propylene carbonate solution by applying external biases for 10 s. The details of the discussion on the poling pretreatment method, particularly the choice of 8 V for poling, are presented in the Supporting Information S5 and S7. As shown in Figure 1 c, after −8 V poling, the BFO electrode has a higher fluorescence intensity than the same electrode that had experienced +8 V pretreatment, revealing that the fluorescent recombination of the photo-generated charges is initiated by the −8 V poling. Poling potentials, particularly the potentials with an exact value larger than the coercive field, re-orientate the distribution of the ferroelectric domains that were differently poled and the direction of internal field is correspondingly tuned.[9,11] As a consequence, the internal field in BFO films points to the BFO surface after being poled by −8 V and a downward band bending is formed at the BFO/air interface or the BFO/electrolyte interface (Figure 1 d, right). In combination with the electron barrier at the ITO/BFO contact, the photo-generated electrons can only be trapped in the bulk of the BFO films and thus recombination with the holes in the valence band becomes the sole way to release the excited energy. On the other hand, a positive pretreatment potential switches the internal field so that it points towards the ITO electrode and give an

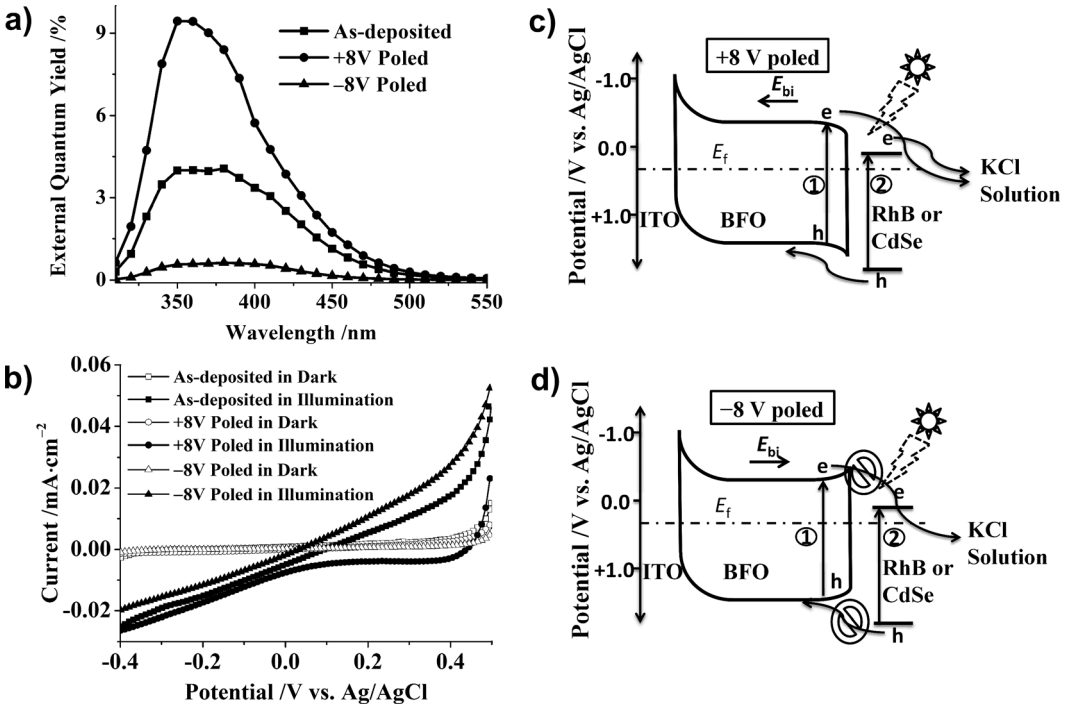

Figure 2. a) External quantum yield spectra measured for BFO electrodes before poling and after +8 V and −8 V poling. b) Photocurrent–potential characteristics of the photoelectrodes with different polarization states. Schematic representations of the mechanisms in photo-excited charge transfer from BFO films to the electrolyte ① and from excited surface modifiers to the BFO films ② after the BFO films were c) positively and d) negatively poled.

upward band bending (Figure 1d; left) which promotes the photo-generated electrons to move to the surface. Considering that the Schottky barrier at BFO/ITO is favorable to drive photo-generated holes efficiently to ITO, the possibility of electron–hole recombination is greatly reduced in this case because of the separation of the charges.

Figure 2a and b show representative steady-state photoelectrochemical data for the BFO/ITO photoelectrodes that have undergone poling pretreatments (+8 V or −8 V) and been immersed in an aqueous solution (0.1M KCl) for measurements. The wavelength-dependent external quantum yield spectra measured without any external bias undoubtedly demonstrate that the polarization states in the ferroelectric films determine the corresponding solar-energy conversion efficiencies. In accordance with the fluorescent analysis, the +8 V poling treatment results in the highest external quantum efficiency owning to the lowest charge recombination rate in comparison with the same electrode experienced no poling or −8 V poling. The external quantum yield of the intrinsic sample is higher than the same sample with −8 V treatment, implying that the ferroelectric domains in the as-grown polycrystalline BFO films are randomly distributed and not optimized. Correspondingly, the photocurrent–potential plots of the as-prepared sample show intermediate results between the positively and negatively poling conditions as illustrated in Figure 2b. To simplify the discussion, we just focus on the investigation of the samples under positively or negatively poling conditions. The external quantum yield of the +8 V poled electrode is almost 10-fold larger than the same sample that underwent −8 V poling, illustrative of an excellent capability for tuning the photocurrent in BFO photoelectrodes. The external quantum yield of the photoelectrode with −8 V poling is lower than 1%. This negligible value is probably from the photo-generated charges at the BFO surface, since the downwards band bending caused by the −8 V poling prevents the electrons from transferring to surface. The profile of these external quantum yield spectra qualitatively matches the absorption spectrum of the BFO films with the value threshold at 500 nm (Figure S1), suggesting that the photo-generated charges in BFO contribute solely to the photocurrent in this case.

The photocurrent–potential plots of the poled BFO photoelectrodes as shown in Figure 2b reveal two distinct features. First, the electrodes both positively and negatively poled, exhibit a cathodic photocurrent, meaning that the photocurrent is formed by the transfer of photo-generated holes rather than the electrons to the ITO/glass. The existence of the 1.24 eV Schottky barrier at BFO/ITO interface is mainly responsible for this feature. Such a barrier obstructs electron but boosts hole transfer to the ITO electrode so that only a cathodic photocurrent is obtained, no matter how the BFO films are poled. Second, the parameters for characterizing the photo response of the BFO electrodes show that they have an impressive tunable capability. At 0 V vs Ag/AgCl, the photocurrent could be switched from around 0 $\mu A\,cm^{-2}$ to 10 $\mu A\,cm^{-2}$ and V_{oc} also has a good variability with the value change from 33 mV to 440 mV, after the poling bias of the ferroelectric electrode is manipulated from −8 V to +8 V. As the scanning potential increases negatively, the photocurrent of the −8 V poled electrode also changes accordingly, that is, becomes more negative. Although the negative scanning potential is smaller than the coercive field and cannot switch the orientation of the remnant polarization, it can still raise the Fermi level of the BFO films, reduce the electron barrier induced by the −8 V poling at the BFO/electrolyte interface and thus cause the leaking of current to the electrolyte. In the whole scanning range, the photocurrent of the −8 V poled electrode is always lower than the same electrode after +8 V poling, indicating that the band bending

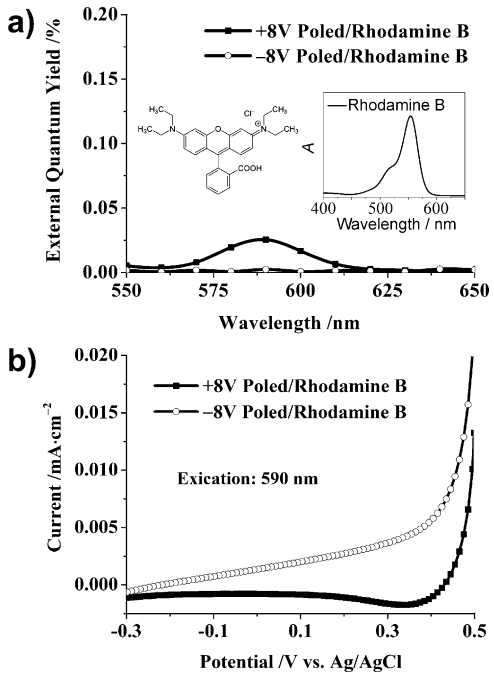

Figure 3. a) External quantum yield spectra of the BFO electrodes measured with 50 μM Rhodamine B. Inset: the absorption spectrum of Rhodamine B in water. b) Photocurrent–potential measurements under a 590 nm illumination (ca. 1 mW cm^{-2}) from a monochromator.

at the BFO/electrolyte interface induced by poling treatment is crucial to the tuning capability of the ferroelectric electrode. The mechanism of the photo-generated charge transfer in BFO is schematically shown as the procedure ① in Figure 2c and d.

The poling treatment could not only adjust the photo-generated charge transfer in BFO films, but could also be of use in tuning the excited charge transfer from the surface modifiers. Separate investigations were carried out to assess how the poling treatment impacted the charge transfer. The steady-state photoelectrochemical data were collected by immersing the ferroelectric photoelectrode in an aqueous solution with 0.1M KCl as the supporting electrolyte and 50 μM Rhodamine B as the modifier. As presented in Figure 3a, the external quantum yield spectra demonstrate that the +8 V poled electrode exhibits a prominent peak at 590 nm and the profile of this peak is in agreement with the absorption spectrum of Rhodamine B (Figure 3a, inset), a result which is strongly indicative that the photocurrent signal measured at wavelengths longer than the band-gap energy of BFO is from the photo-excited hole injection of Rhodamine B. When the ferroelectric photoelectrode is poled at −8 V, the external quantum yield peak from Rhodamine B disappears. To support this observation, photocurrent–potential measurements were conducted under 590 nm illumination (ca. 1 mW cm^{-2}) from a Newport monochromator. Consistent with the external quantum yield measurements, the +8 V poled electrode shows an clear cathodic photocurrent while no cathodic photocurrent is observed for the same electrode with −8 V poling (Figure 3b). The position of the BFO valence band is reported to be around 1.5 V vs the normal hydrogen electrode (NHE),[28,29] higher than the highest occupied molecular orbital (HOMO) position of Rhodamine B.[4] As shown in Figure 2c,d, the consequent band gap alignment for BFO/Rhodamine B is favorable for the excited hole injection from Rhodamine B to BFO films. Once the excited holes are captured at the surface of the BFO films, the poling-induced band bending determines the transfer of the injected holes. The upward band bending by +8 V poling drives the holes to the bulk of the BFO films and forms an sensitization photocurrent collected by the ITO electrode. The downward band bending by −8 V poling, however, inhibits the movement of the holes to the bulk of the BFO film and the holes could only be trapped at the BFO films surface thus no sensitization photocurrent is observed. This novel charge-transfer switching ability is also occurs for other triphenylmethane dyes, such as Rose Bengal and Brilliant Green as demonstrated in Figure S5.

Figure 4a illustrates the representative external quantum yield spectra of the BFO electrodes sensitized with CdSe quantum dots and measured in an aqueous solution with 0.1M KCl. The XRD pattern and TEM image in Figure 4b confirm that the prepared nanoparticles are 4.5 nm CdSe quantum dots. To adsorb quantum dots, the BFO electrodes were soaked in a hexanes solution with 10 mg mL^{-1} oleic acid capped CdSe quantum dots for 10 min, rinsed with hexanes, immersed in a methanol solution with excess ethylenediamine for ligand exchange, and finally placed in the aqueous test electrolyte for analysis. In Figure 4a, the +8 V poled BFO/CdSe exhibits a pronounced photocurrent signal unlike the −8 V poled counterpart beyond the absorption threshold of BFO. The well matched profile of the external quantum yield spectrum with the absorption spectrum of the 4.5 nm CdSe

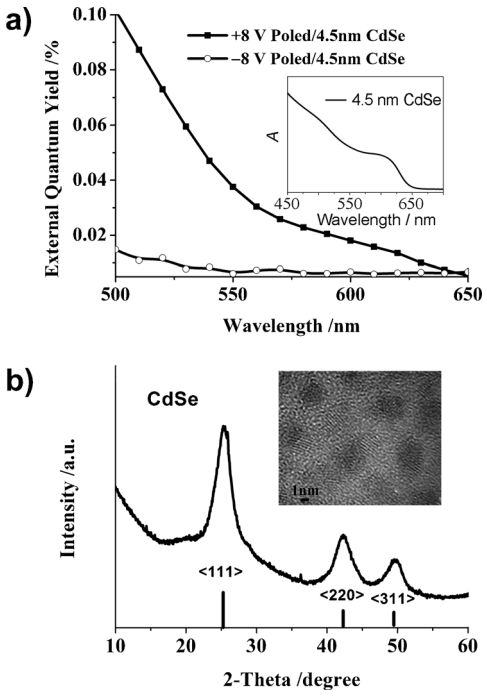

Figure 4. a) External quantum yield spectra of the BFO electrodes sensitized with CdSe quantum dots. Inset: Absorption spectroscopic measurements of CdSe quantum dots in hexanes . b) XRD pattern of CdSe quantum dots. Inset: TEM image of CdSe quantum dots.

quantum dots (Figure 4a), suggests that the photo-excited hole injection from CdSe quantum dots contributes to the increased external quantum yield. For the −8 V poled BFO/CdSe, no photocurrent beyond the BFO absorption threshold is observed, confirming that the charge injection from quantum dots could also be switched by the poling pretreatment of the ferroelectric electrodes. Considering the large depolarization electric field across the ferroelectric film, the observation of the excited hole injection from inorganic quantum dots to positively poled BFO films supports the idea that ferroelectric photoelectrodes could be alternative platforms to extract multiple holes (electrons) generated from one absorbed photon or hot holes (electrons) in quantum dots without losing any photovoltage, though more research needs to be made.

The cumulative experimental results illustrate an alternative design strategy for constructing smart photoelectrochemical systems with a good switchable capability for charge transfer. Specifically, the BFO photoelectrodes offer advantages that differ from those of conventional semiconductor photoelectrodes. The switchable band bending at the surface of the ferroelectric electrodes could be utilized to drive both reduction and oxidation reactions according to the orientation of the remnant polarization. Additionally, such reactions are not limited to the photon assisted reactions such as water splitting, but common electrochemical reactions could also be tuned by the poling treatments of the ferroelectric electrodes.[30] With regards to the photoelectrochemical energy conversion, the tunability of the charge transfer in the ferroelectric photoelectrode broadens the possibility to design a complete photoelectrochemical cell with only ferroelectric electrodes that behave as photoanodes or photocathodes relying on the choice of poling biases. Although it was not a primary focus of this study, these data also imply that the BFO photoelectrodes still have a pounced external quantum efficiency by considering the relatively poor ferroelectric performance in comparison with single crystalline BFO films.[8] Additional progress in the spin-coating technique for improving the ferroelectric performance of BFO should be made, to utilize the orientation of the ferroelectric domains maximally and to harvest the excited charges or even hot charges from quantum dots efficiently.

In summary, cost-advantageous polycrystalline BFO photoelectrodes were fabricated using a typical spin-coating technology. Their distinct ferroelectric performance allows the orientations of the BFO band bending at the BFO/electrolyte to be switched from upwards to downwards by poling pretreatments. Accordingly, charge-transfer directions of photo-exited charges either generated in the BFO or in the surface modifiers, such as molecular dyes and CdSe quantum dots were tuned, as demonstrated by the systematical steady-state photoelectrochemical investigations. These results therefore, makes it possible to manipulate photoelectrochemical reactions on a single ferroelectric photoelectrode and provides insight on strategies for designing smart photoelectrochemical systems.

Received: June 9, 2014
Published online: August 22, 2014

Keywords: $BiFeO_3$ · charge transfer · photoelectrodes · polarization · tunability

[1] D. M. Chapin, C. S. Fuller, G. L. Pearson, *J. Appl. Phys.* **1954**, *25*, 676 – 678.
[2] J. Britt, C. Ferekides, *Appl. Phys. Lett.* **1993**, *62*, 2851 – 2852.
[3] B. O'Regan, M. Grätzel, *Nature* **1991**, *353*, 737 – 740.
[4] M. Chitambar, Z. Wang, Y. Liu, A. Rockett, S. Maldonado, *J. Am. Chem. Soc.* **2012**, *134*, 10670 – 10681.
[5] M. A. Green, K. Emery, Y. Hishikawa, W. Warta, E. D. Dunlop, *Prog. Photovoltaics* **2013**, *21*, 827 – 837.
[6] M. A. Green, K. Emery, Y. Hishikawa, W. Warta, E. D. Dunlop, *Prog. Photovoltaics* **2014**, *22*, 1 – 9.
[7] H. Taniguchi, A. Kuwabara, J. Kim, Y. Kim, H. Moriwake, S. Kim, T. Hoshiyama, T. Koyama, S. Mori, M. Takata, et al., *Angew. Chem.* **2013**, *125*, 8246 – 8250; *Angew. Chem. Int. Ed.* **2013**, *52*, 8088 – 8092.
[8] W. Ji, K. Yao, Y. C. Liang, *Adv. Mater.* **2010**, *22*, 1763 – 1766.
[9] H. T. Yi, T. Choi, S. G. Choi, Y. S. Oh, S.-W. Cheong, *Adv. Mater.* **2011**, *23*, 3403 – 3407.
[10] A. Bhatnagar, A. Roy Chaudhuri, Y. Heon Kim, D. Hesse, M. Alexe, *Nat. Commun.* **2013**, *4*, 2835.
[11] T. Choi, S. Lee, Y. J. Choi, V. Kiryukhin, S.-W. Cheong, *Science* **2009**, *324*, 63 – 66.
[12] D. Cao, C. Wang, F. Zheng, W. Dong, L. Fang, M. Shen, *Nano Lett.* **2012**, *12*, 2803 – 2809.
[13] D. Cao, J. Xu, L. Fang, W. Dong, F. Zheng, M. Shen, *Appl. Phys. Lett.* **2010**, *96*, 192101.
[14] C. Wang, D. Cao, F. Zheng, W. Dong, L. Fang, X. Su, M. Shen, *Chem. Commun.* **2013**, *49*, 3769 – 3771.
[15] J. M. Frost, K. T. Butler, F. Brivio, C. H. Hendon, M. van Schilfgaarde, A. Walsh, *Nano Lett.* **2014**, *14*, 2584 – 2590.
[16] J. Lee, S. Esayan, J. Prohaska, A. Safari, *Appl. Phys. Lett.* **1994**, *64*, 294.
[17] L. Pintilie, M. Lisca, M. Alexe, *Appl. Phys. Lett.* **2005**, *86*, 192902.
[18] S. Y. Yang, J. Seidel, S. J. Byrnes, P. Shafer, C.-H. Yang, M. D. Rossell, P. Yu, Y.-H. Chu, J. F. Scott, J. W. Ager, et al., *Nat. Nanotechnol.* **2010**, *5*, 143 – 147.
[19] D. Lee, S. H. Baek, T. H. Kim, J.-G. Yoon, C. M. Folkman, C. B. Eom, T. W. Noh, *Phys. Rev. B* **2011**, *84*, 125305.
[20] W. Ji, K. Yao, Y.-F. Lim, Y. C. Liang, A. Suwardi, *Appl. Phys. Lett.* **2013**, *103*, 062901.
[21] Z. L. Wang, W. Wu, *Angew. Chem.* **2012**, *124*, 11868 – 11891; *Angew. Chem. Int. Ed.* **2012**, *51*, 11700 – 11721.
[22] F. Gao, X. Y. Chen, K. B. Yin, S. Dong, Z. F. Ren, F. Yuan, T. Yu, Z. G. Zou, J.-M. Liu, *Adv. Mater.* **2007**, *19*, 2889 – 2892.
[23] S. K. Singh, H. Ishiwara, K. Maruyama, *Appl. Phys. Lett.* **2006**, *88*, 262908.
[24] H. Lee, Y. S. Kang, S.-J. Cho, B. Xiao, H. Morkoç, T. D. Kang, G. S. Lee, J. Li, S.-H. Wei, P. G. Snyder, et al., *J. Appl. Phys.* **2005**, *98*, 094108.
[25] S. Saha, T. Sinha, A. Mookerjee, *Phys. Rev. B* **2000**, *62*, 8828 – 8834.
[26] S. Y. Yang, L. W. Martin, S. J. Byrnes, T. E. Conry, S. R. Basu, D. Paran, L. Reichertz, J. Ihlefeld, C. Adamo, A. Melville, et al., *Appl. Phys. Lett.* **2009**, *95*, 062909.
[27] R. Schafranek, S. Payan, M. Maglione, A. Klein, *Phys. Rev. B* **2008**, *77*, 195310.
[28] B. C. Huang, Y. T. Chen, Y. P. Chiu, Y. C. Huang, J. C. Yang, Y. C. Chen, Y. H. Chu, *Appl. Phys. Lett.* **2012**, *100*, 122903.
[29] Z. Liu, F. Yan, *Phys. Status Solidi RRL* **2011**, *5*, 367 – 369.
[30] P. M. Jones, D. E. Gallardo, S. Dunn, *Chem. Mater.* **2008**, *20*, 5901 – 5906.

